N. Rodriguez Rodriguez, L. Machiels, K. Binnemans
ACS Sustainable Chemistry & Engineering **7**, 3940–3948 (2019).
DOI: 10.1021/acssuschemeng.8b05072

p-Toluenesulfonic Acid-Based Deep-Eutectic Solvents for Solubilizing Metal Oxides

Nerea Rodriguez Rodriguez[a,b], Lieven Machiels[a], Koen Binnemans[a]*

[a] KU Leuven, Department of Chemistry, Celestijnenlaan 200F, P.O. Box 2404, B-3001 Leuven (Belgium).

[b] SIM vzw, Technologiepark 935, B-9052 Zwijnaarde (Belgium).

*Corresponding author:

e-mail: Koen.Binnemans@kuleuven.be; Phone: +32 16 32 7446

Abstract

Combinations of *p*-toluenesulfonic acid monohydrate with different hydrogen-bond acceptors (i.e., choline chloride, tetraethylammonium chloride, tetrabutylammonium chloride, betaine hydrochloride, β-alanine, tetrabutylphosphonium chloride, ethylammonium chloride, methyltriphenylphosphonium bromide, and benzyltriphenylphosphonium chloride) were tested for deep-eutectic solvent (DES) formation. Only *p*-toluenesulfonic acid monohydrate:choline chloride, *p*-toluenesulfonic acid monohydrate:tetrabutylammonium chloride, and *p*-toluenesulfonic acid monohydrate:tetrabutylphosphonium chloride at a 1:1 molar ratio remained liquid at room temperature. The obtained deep-eutectic solvents were characterized by determining their density and viscosity as function of temperature, and their thermal operational window (i.e., decomposition temperature and melting point/glass transition temperature). Moreover, IR spectroscopy was used to elucidate the formation of hydrogen bonds. The solubility of different metal oxides in the DES *p*-toluenesulfonic acid monohydrate:choline chloride was experimentally determined. The effect of the hydrogen-bond donor:hydrogen-bond acceptor molar ratio (2:1, 1:1, and 1:2) on the metal oxide solubility was explored. A comparison was made with metal oxide solubilities in other choline chloride-based DESs and in acidic aqueous solutions.

Keywords: Deep-eutectic solvents; ionic liquids; metal oxides; solvometallurgy; *p*-toluenesulfonic acid monohydrate.

Introduction

The production of metals from ores has been generally carried out via pyrometallurgical and hydrometallurgical processes. However, in the recent years a new branch of metallurgy has emerged as a promising alternative: solvometallurgy.[1] Conceptually, solvometallurgy is analogous to hydrometallurgy, both in terms of unitary operations and operational conditions. However, instead of aqueous acidic or alkaline solutions, solvometallurgy uses non-aqueous solvents, such as molecular organic solvents, ionic liquids (ILs), and deep-eutectic solvents (DESs).[2–4] The main advantage of solvometallurgy over other types of metallurgy is its higher selectivity and lower water consumption, which could be potentially applied for the treatment of low grade ores.[1] Solvometallurgy with ILs and DESs is also termed ionometallurgy.[5–8]

The extraction of metals from low grade ores is a challenging task due to the large variety of sources: oxides, sulfides, carbonates, phosphates, or silicates. Metal oxides are insoluble in most molecular solvents, and very acidic or basic conditions are required. ILs have been proposed as promising alternative solvents for the solubilization of metal oxides.[9–16] However, their high price, generally attributed to a complex synthesis process, is the main disadvantage for their industrial-scale implementation. The preparation of DESs is done by mixing readily available bulk components, which is easier and less expensive. Their physicochemical properties are similar to ILs, including a negligible vapor pressure and a broad thermal operational window. Generally, DESs are composed of quaternary ammonium or phosphonium salts acting as hydrogen-bond acceptors (HBAs) complexed with hydrogen-bond donors (HBDs) such as amides, polyols, or carboxylic acids. The properties of both types of solvents can be modified by changing the HBD-HBA combination, and the HBD:HBA molar ratio.

In recent years, DESs have also been proposed as alternative solvents for the solubilization of metal oxides.[17–19] It has been reported that choline chloride-based DESs can solubilize a broad range of metal oxides, but the solubility is largely dependent on the selected HBD. In fact, this effect is so remarkable that the modification of the HBD can induce changes in the solubility of up to several orders of magnitude. These differences in solubility can be exploited for selective leaching or metal oxides processing. In general, it was found that the majority of the transition metals are soluble in the different DESs, but the more covalent metal oxides (e.g., aluminates and silicates) are insoluble in all DESs studied to date.[19] Different HBDs have been investigated (ethylene glycol,[17] urea[17,18] and carboxylic acids[17,19]), and the highest solubilities of metal oxides were found when carboxylic acids were used as HBD, e.g., malonic acid and oxalic acid.[17–19] When the solubility data of the metal oxides in the DES malonic acid:choline

chloride(1:1) were compared to that in HCl, a correlation was found, but not when compared to those of NaCl, showing that the solubility was not purely related to the presence of chloride ions. Nonetheless, no metal-containing cationic species were identified, and the anionic species that were identified were chlorometalate species of the form MCl_x^-. The higher solubilities of the oxides in HCl and malonic acid were attributed to the presence of protons, which act as oxide acceptors and change the formed complex.[17]

To develop DESs with an enhanced metal oxide solubility via an increase in acidity of the HBD, we considered *p*-toluenesulfonic acid monohydrate (ptsa) as HBD (Figure 1). The synthesis of ptsa is performed via direct sulfonation of toluene.[20] It is used in a very broad range of applications, e.g., as a catalyst, detergent solubilizer, resin hardener, in pharmaceuticals, or as an intermediate in the production of saccharine.[21,22] In the literature, different ptsa-based DESs have already been reported, but barely characterized, e.g., ptsa:choline chloride at a molar ratio of 1:1, ptsa:benzyltrimethylammonium chloride at a molar ratio of 2.3:1, ptsa: allyltriphenylphosphonium bromide at a molar ratio 3:1, or ptsa:n,n-diethylenethanol ammonium chloride.[23–31] In this paper, combinations of ptsa with different HBAs were prepared in a 1:1 molar ratio, in order to obtain ptsa-based eutectic mixtures. The mixtures that resulted in a DESs were physicochemically characterized. The HBD:HBA combination ptsa:ChCl was selected for the experimental determination of the solubility of different metal oxides. The effect of the HBD:HBA ratio on both the physicochemical properties of the mixture, and the solubility of metal oxides have been investigated.

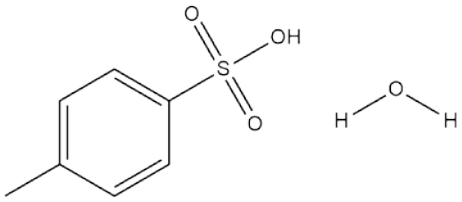

Figure 1: Structure of *p*-toluenesulfonic acid monohydrate

Experimental procedure

Chemicals

The chemicals used in this work were purchased from trustful sources, and used as received without further purification. Choline chloride (99 wt%), *p*-toluenesulfonic acid monohydrate (97.5 wt%), betaine hydrochloride (99 wt%), benzyltriphenylphosphonium chloride (99 wt%), manganese(IV) oxide (88 wt%), and lead(IV) oxide (97wt%) were purchased from Acros Organics. Tetraethylammonium chloride (>98 wt%), tetrabutylammonim chloride (97 wt%), *β*-alanine (98 wt%), ethylamine hydrochloride (98 wt%), methyltriphenylphosphonium bromide (98 wt%), manganese(II) oxide (99 wt%), iron(III) oxide (>99 wt%), iron(II, III) oxide (>95 wt%), copper(II) oxide (>99 wt%), and lead(II) oxide (>99 wt%) were purchased from Sigma-Aldrich. Tetrabutylphosphonium chloride (>95 wt%) was obtained from Io-Li-Tec. Cobalt(II, III) oxide (P.A. grade) was obtained from UCB, zinc oxide (P.A. grade) from Merck, indium(III) oxide(99.9 wt%) from Alfa Aesar. Standard solutions of manganese, iron, cobalt, copper, zinc, indium and lead [1000 μg mL^{-1}] were purchased from Sigma Aldrich.

Preparation and characterization of the DESs

The DESs were prepared via the heating method, i.e, the HBD and HBA were weighed, placed in 40 mL glass screw cap vials, and heated to 80 °C while stirring until a clear liquid was formed. The mixtures were heated in a sand bath using a magnetic stirrer (IKA RCT basic) with temperature controller (VWR VT-5). The HBD:HBA combinations that formed a clear liquid after heating were left at room temperature for 24 h. Only those mixtures which remained liquid after cooling were further characterized. The water content of the DESs was measured using a volumetric Karl Fischer titrator (Mettler-Toledo DL38). The density and viscosity as a function of the temperature were measured using an Anton Paar Lovis 2000 M/ME rolling-ball viscometer. The decomposition temperature was measured using a TA Q500 thermogravimetric analyzer. The samples were heated from 30 °C to 400 °C at a heating rate of 5°C·min^{-1} in a 60mL·min^{-1} N_2 flow. Melting points or glass transitions were determined with a differential scanning calorimetry, Mettler-Toledo DSC822e module. The DSC method used was the following: cooling from 35 °C to -80 °C at a cooling rate of 5 °C·min^{-1}, isotherm at -80 °C for 30 minutes, and heating to 35 °C at a heating rate of 2 °C min^{-1}, for two cycles in helium atmosphere. Infrared spectra were measured on a Bruker Vertex 70 FTIR spectrometer, with an ATR sample holder.

Dissolution of metal oxides

The solubility of different metal oxides (MnO, MnO_2, Fe_2O_3, Fe_3O_4, Co_3O_4, CuO, Cu_2O, ZnO, In_2O_3, PbO, PbO_2,) in the DESs ptsa:ChCl(2:1), ptsa:ChCl(1:1), and ptsa:ChCl(1:2) was experimentally determined by following a procedure previously reported in the literature.[17,18] An excess of metal oxide (approximately 0.1 g) was mixed with 2 mL of DES for 24 h 50 °C and 500 rpm using a magnetic stirrer (IKA RCT basic) with temperature controller (VWR VT-5). In some cases, 0.1 g were fully dissolved in very short time, in those cases extra metal oxide was added to the vial (up to 0.3 g). The solution was subsequently filtered using syringe filters (pore size 0.45 µm). The metal concentration of the filtered sample was determined by Inductively Coupled Plasma Optical Emission Spectroscopy (ICP-OES) using a Perkin-Elmer Optima 8300DV device. The filtered samples were diluted in a nitric acid solution (2 vol%), with the exception of the Cu_2O samples which were diluted in a hydrochloric acid solution (4 vol%), to avoid the precipitation of Cu. The samples were diluted between 100 and 2000 times, to have a final metal concentration lower than 50 ppm, suitable for the ICP-OES measurement. In order to minimize the error, two serial dilutions were performed. Niobium (5ppm) was used as internal standard. The selected spectral lines (in nm) for quantification were: Co 228.616, Cu 324.752, Fe 238.204, In 230.606, Mn 257.610, Ni 221.648, Pb 217.000, and Zn 206.200. All the solubility experiments were done in triplicate.

Results and discussion

Preparation of DESs

In order to find highly acidic DESs for solvometallurgical applications, ptsa was mixed with different HBAs (always in a molar ratio 1:1). The selected HBAs were: (1) choline chloride, (2) tetraethylammonium chloride, (3) tetrabutylammonium chloride, (4) betaine hydrochloride, (5) β-alanine, (6) tetrabutylphosphonium chloride, (7) ethylammonium chloride, (8) methyltriphenylphosphonium bromide, and (9) benzyltriphenylphosphonium chloride.

From the nine studied HBD:HBA combinations (in a 1:1 molar ratio), five formed a clear liquid upon heating: (1) ptsa:choline chloride (previously reported in the literature),[24,32,33] (2) ptsa:tetraethylammonium chloride, (3) ptsa:tetrabutylammonium chloride, (4) ptsa:tetrabutylphosphonium chloride, and (5) ptsa:ethylammonium chloride. However, only ptsa:choline chloride (ptsa:ChCl(1:1)), ptsa:tetrabutylammonium chloride (ptsa:tbaCl(1:1)), and ptsa:tetrabutylphosphonium chloride (ptsa:tbpCl(1:1)) remained liquid at room temperature after 24 h. The industrial applicability of DESs with melting point higher than room temperature

is compromised due to the costs associated to continuous heating. Therefore, only the three DESs with melting point lower than room temperature were considered for further studies. In Figure 2, the formed DESs which remained liquid at room temperature are shown.

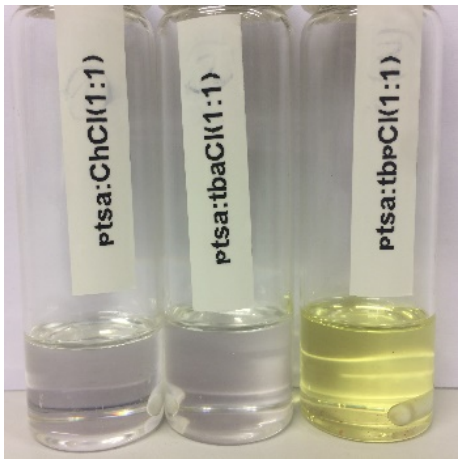

Figure 2: Selected DESs with melting point lower than room temperature

Characterization of the deep-eutectic solvents

The DESs ptsa:ChCl(1:1), ptsa:tbaCl(1:1), and ptsa:tbpCl(1:1) have been characterized in order to study the effect of the HBA type on the physical properties of the DESs. Besides, the DESs ptsa:ChCl(2:1), ptsa:ChCl(1:2) have also been and characterized to investigate the effect of the HBD:HBA molar ratio on the physical properties of the DESs. The obtained results are discussed below.

Density

The density of the selected DESs was measured in a temperature range from 35 to 60 °C and at atmospheric pressure. The obtained density values are depicted in Figure 3 (effect of the HBA type) and Figure 4 (effect of the HBD:HBA molar ratio), and tabulated in the Supporting Information (SI) in Table S1. The water content of the DESs is also included in Table S1.

The density follows a linear trend with the temperature, which can be expressed using Equation 1:

$$\rho\left(\frac{g}{cm^3}\right) = a + b \cdot T(K) \qquad (1)$$

where ρ is the density in g/cm^3, T is the temperature in K and a and b are adjustable parameters. The adjustable parameters and standard deviation are shown in Table S2.

From Figure 3 and Figure 4 it can be observed that the density of the studied DESs decreases linearly over the studied temperature interval. From Figure 3, it can be observed that the density decreases in the following order: ptsa:ChCl(1:1) > ptsa:tbpCl(1:1) > ptsa:tbaCl(1:1). A comparison between the density values of ptsa:tbpCl(1:1) and ptsa:tbaCl(1:1) revealed that the central atom of the HBA has a rather limited effect on the density of the DES. Nonetheless, the substitution of the N atom by a heavier atom, i.e. a P atom, results in a slight increase in density. This behavior was reported previously for DESs based on ethylene glycol as HBD. Furthermore, it was observed that the effect of the HBA alkyl chain length/symmetry on the density was much more pronounced than the effect of the central atom. It was found that the density decreases with the cation alkyl chain length/symmetry, i.e., ptsa:ChCl(1:1) > ptsa:tbaCl(1:1). The elongation of the alkyl chain length increases the free volume, resulting in a lower overall density.[34] Both observations are in agreement with literature.[35,36]

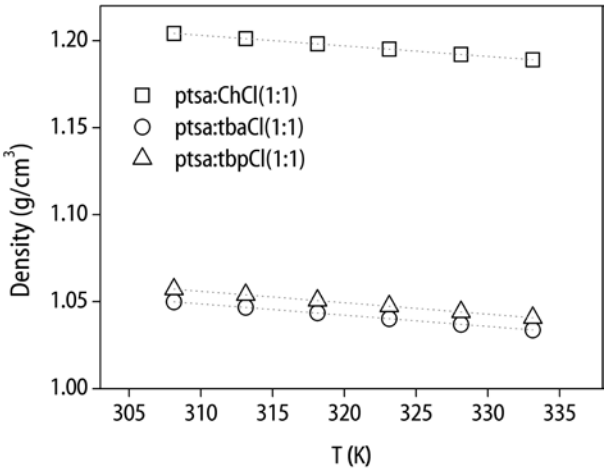

Figure 3: Density as a function of temperature for the DESs ptsa:ChCl (□), ptsa:tbaCl (○), and ptsa:tbaCl (△), and fitted values (dotted line).

The effect of the HBD:HBA molar ratio on the density is shown in Figure 4. From Figure 4 it can be observed that the density of the investigated DESs increases in the following order: ptsa:ChCl(1:2) < ptsa:ChCl(1:1) < ptsa:ChCl(2:1), meaning that the density decreases with the salt concentration. This behavior is agreement with the literature, and it can be attributed to an increase free molar volume produced by the increase in salt concentration.[35,37]

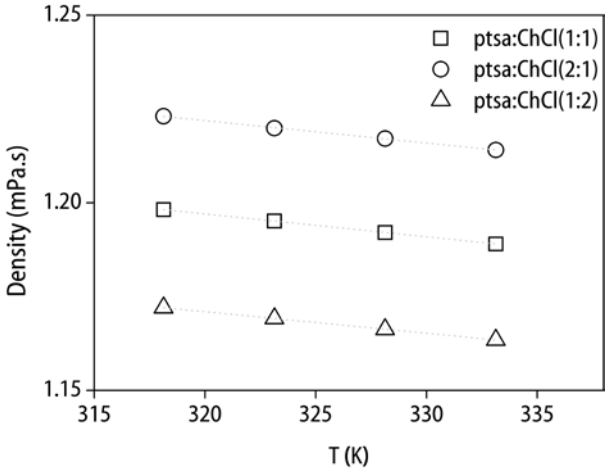

Figure 4: Density as a function of temperature for the DESs: (□) ptsa:ChCl (1:1); (○), and ptsa:ChCl (2:1), and (△) ptsa:ChCl(1:2), and fitted values (dotted line).

Viscosity

The viscosity of the selected DESs was measured in a temperature range from 35 to 60 °C and at atmospheric pressure. The obtained values are depicted in Figure 5 and Figure 6, and tabulated in Table S3.

The viscosity as a function of temperature can be adjusted according to the Vogel-Fulcher-Tamman (VTF) equation, which is presented in equation 2:

$$\eta = A \cdot \exp\left(\frac{B}{T - T_0}\right) \quad (2)$$

where A (mPa·s), B (K) and T_0 (K) are the fitting parameters. The adjustable parameters and standard deviation are shown in Table S4.

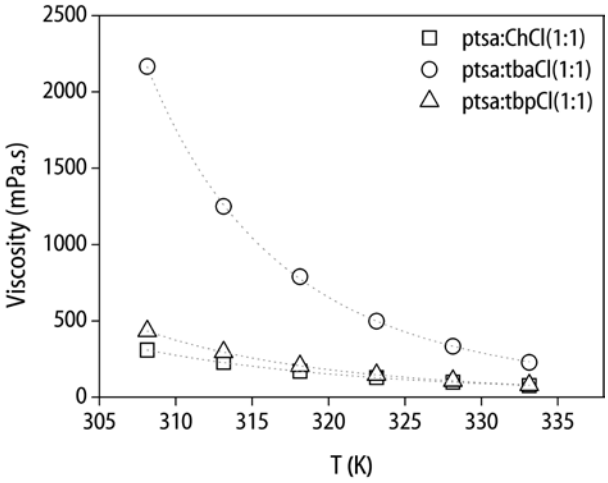

Figure 5: Viscosity as a function of temperature for ptsa:ChCl (□), ptsa:tbaCl (○), and ptsa:tbaCl (△), and fitted values (dotted line).

From Figure 5 and Figure 6 it can be observed that, like most ILs and DESs, the viscosity-temperature profile can be satisfactorily fitted to the VFT equation (fitting parameters can be found in the SI). From Figure 5, the effect of the HBA on the viscosity of the DESs can be investigated. The viscosity of the three studied DESs decreases in the following order ptsa:tbaCl(1:1) >> ptsa:tbpCl(1:1) > ptsa:ChCl(1:1). The viscosity can be related to the strength of the molecular interactions of the fluid. It was found that, in contrast to the density, an increase in alkyl chain length/symmetry of the cation increases the viscosity. The observed behavior is in agreement with the higher resistance to flow due to the increase of the dispersive interactions.[36] It was also found that for HBDs with the same alkyl chain length, the viscosity of the phosphonium-based DES is lower than that of the ammonium-based DES. This behavior is also observed for ILs, and it has been attributed to the larger molar volume of the phosphonium, which lowers the cation charge density and weakens interionic interactions.[38–40] The viscosities of the studied ptsa-based DESs can be considered low compared to those of other DESs formed by quaternary ammonium salts and carboxylic acids. This is of great importance in terms of industrial applicability. A comparative graph can be found in the SI (Figure S1).[41]

From Figure 6 it is observed that the viscosity increases in the following order: ptsa:ChCl(2:1) < ptsa:ChCl(1:1) < ptsa:ChCl(1:2), meaning that the viscosity increases with the salt concentration. The lower the salt concentration, the weaker the electrostatic interactions of the

anion with the different components and thus, the viscosity. This behavior has been observed for other ChCl-based DESs, with the exception of those using glycerol as HBD.[35,37]

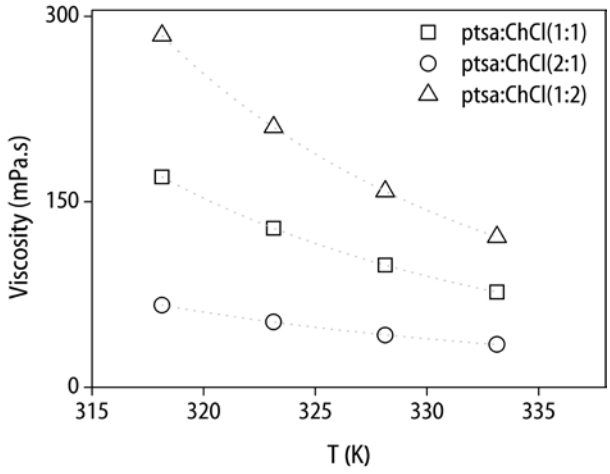

Figure 6 : Viscosity as a function of temperature for the DESs: (□) ptsa:ChCl (1:1); (○), and ptsa:ChCl (2:1), and (△) ptsa:ChCl(1:2), and fitted values (dotted line).

Decomposition temperature and melting point

The thermal operational window of the selected DESs was experimentally determined via thermogravimetric analysis (TGA) and differential scanning calorimetry (DSC). The thermal decomposition temperature is strongly influenced by the experimental conditions, e.g. heating rate, pressure, surrounding environment and water content of the sample. The same method was used for all the samples and is described in the experimental procedure section. The experimentally determined decomposition temperatures are presented in Table 1 and Figure 7. In Figure 7 it can be observed that the thermal decomposition of the ptsa-based DESs occurred during two well differentiated processes. Firstly, a desorption/drying region was observed, where a large mass loss was followed by a plateau. This behavior is associated with the evaporation of a volatile component, namely water. Secondly, a typical single stage decomposition curve was observed. As expected, the mass loss associated to the drying process is more pronounce with increasing amounts of ptsa (i.e., higher water contents). The values of the decomposition temperature reported in Table 1 correspond to the onset value of the decomposition curve. For the DESs with different HBA, the decomposition temperature decreased in the order: ptsa:tbpCl(1:1) >> ptsa:ChCh(1) > ptsa:tbaCl(1:1). For the ChCl-based DESs, the decomposition temperature of the studied DESs decreases in the following order:

ptsa:ChCl(1:1) > ptsa:ChCl(2:1) > ptsa:ChCl(1:2). Therefore, contrary to what it would be expected, the decomposition temperature is not proportional to the HBD:HBA ratio.

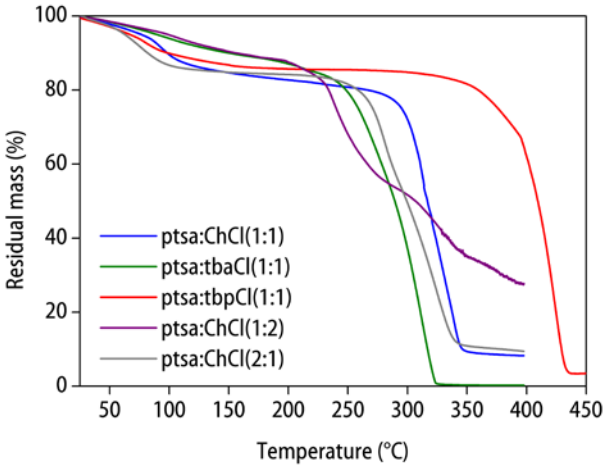

Figure 7: Dynamic TGA analysis of the investigated DESs.

From the DSC measurements, no melting points were observed for any of the studied DESs. This behavior is common for ILs and DESs.[42] At the selected experimental conditions, a glass transition has been observed for ptsa:tbaCl(1:1), ptsa:tbpCl(1:1), and ptsa:ChCl(2:1) (Table 1) but not for ptsa:ChCl(1:1) and ptsa:ChCl(1:2). The experimental glass transition temperatures, corresponding to the onset value of the glass transition peak, are included in Table 1. The glass transition of the DES ptsa:ChCl(1:1) is expected at temperatures lower than -80 °C. The lower melting point/glass transition of the DES ptsa:ChCl(1:1) can be explained on the basis of the lower symmetry of ChCl compared to tbaCl and tbpCl.[43,44] Therefore, for the DESs with the same HBD:HBA molar ratio but different HBA, the melting point of the studied DESs would follow the order: ptsa:ChCl (1:1) < ptsa:tbpCl(1:1) < ptsa:tbaCl(1:1); which is the same trend found for the viscosity, and could also be related to the strength of the intermolecular interactions (i.e., stronger intermolecular interactions lead to higher viscosities and melting points). The effect of the HBD:HBA molar ratio on the melting point cannot be discussed on the basis of the obtained experimental data.

Table 1: Decomposition temperature (T_{decomp}) and glass-transition temperature (T_g) of the DESs ptsa:ChCl(1:1), ptsa:tbaCl(1:1), and ptsa:tbpCl(1:1). The melting temperature (T_m) of the initial components (HBD and HBA) is also included.

DES	T_{decomp} [°C]	T_g [°C]	T_m HBD [°C]	T_m HBA [°C]
ptsa:tbaCl(1:1)	274	-42	103	83
ptsa:tbpCl(1:1)	396	-48	103	62
ptsa:ChCl(1:1)	299	-	103	302
ptsa:ChCl(2:1)	272	12	103	302
ptsa:ChCl(1:2)	224	-	103	302

Spectroscopic studies

The decrease in melting point of the DESs compared to their initial components (Table 1) is generally attributed to the formation of extensive hydrogen-bond networks between the HBD and the HBA. In this work, a decrease of more than 100 °C was found in all the studied combinations. Fourier-transform infrared spectroscopy (FTIR) was used to analyze this behavior.[45,46] After band assignments in the spectra of the pure components, the main changes in the spectra after DES formation gave information on the new interactions formed. The FTIR spectra of the pure components, as well as the spectra of the formed DESs, are presented in the SI (Figure S2-Figure S4).

The IR spectrum of *p*-toluenesulfonic acid monohydrate has been extensively discussed in the literature.[47–49] This spectrum is composed of intense bands in the fingerprint region, representative of the symmetric and asymmetric stretching of SO_3^-, and diffuse absorption bands in the region of 1600-2500 cm^{-1} (H_3O^+). On account of the strong hydrogen bond between SO_3^- and H_3O^+ ions, the indicated bands are substantially broadened. The antisymmetric SO_3 stretching motions appear at 1170 and 1098 cm^{-1}, while the symmetric SO_3 stretch (with significant contribution of the out-of-plane C-H bending motion) appears at 1003 cm^{-1}. The C-S bending motion is found at 1031 cm^{-1}. A more detailed peak assignment can be found elsewhere.[48]

The IR spectrum of the choline chloride shows the OH stretching mode at 3219 cm^{-1}, and the C-H stretching band at 2924 and 3005 cm^{-1}. According to the literature, wavenumbers of the most important absorption bands of the quaternary ammonium salts are as follows: the $N^+(CH_3)_3$ symmetric and asymmetric stretching bands appear at 3020 and 920–930 cm^{-1},

respectively, and the asymmetric bending mode appears at 950 cm^{-1}.[50] Nonetheless, the identification of these bands in the finger print region is hindered by possible band overlap. Similarly, the band assignment of tetrabutylphosphonium chloride is to be done in the fingerprint region, where most of the peaks overlap. The only exceptions are the C-H stretching bands were found at 2957 and 2871cm^{-1}, and the broad absorbance between 3600 and 3350 cm^{-1} due to $Cl^{-}\cdots H\text{-}O\text{-}H\cdots Cl^{-}$, which are also typically observed in quaternary ammonium salts.[51]

The formation of a hydrogen-bond after the combination of ChCl with *p*-toluenesulfonic acid produces changes in the infrared spectra, more specifically broadening and shifting of the bands. In Figure 8, the spectra of the DES ptsa:chCl(1:1) is compared to those of the initial components in the regions of the OH stretching (top), and of the H_3O^+ diffuse absorption bands (bottom). It is observed that upon DES formation, the peak corresponding to the OH region is decreased in intensity, broadened, and shifted to a higher wavenumber region. This behavior was attributed to several factors. The broadening of the peak indicates that the OH group is now involved in a more extensive hydrogen-bonding network.[52] The shift of the OH peak to a higher wavenumber indicates OH hydrogen-bonded groups with a weaker hydrogen-bond strength than those present in the pure component. This behavior has been previously reported in literature. [46,53] In Figure S5, the spectra of the DESs ptsa:ChCl(2:1), ptsa:chCl(1:1), and ptsa:ChCl(1:2) are compared to those of the initial components in the regions of the OH stretching (left), and of the H_3O^+ diffuse absorption bands (right). It has been found that for the same DESs, the higher the concentration of ptsa, the more shifted is the peak. For all the investigated DESs, the diffuse absorption bands associated to H_2O are remarkably broadened. The broadening of the peaks is similar for the three ratios, but the transmittance is proportional to the amount of ptsa. From Figure 9 (top), it can also be observed how the diffuse absorption bands associated to H_2O are remarkably broadened and even disappearing upon the DES formation. This behavior indicates that the H_3O^+ ions previously interacting only with the sulfonic acid, are now involved in hydrogen-bond networks with the HBA. The same behavior was observed for the DESs formed by the mixture of tetrabutylammonium chloride and tetrabutylphosphonium chloride (Figure 9).

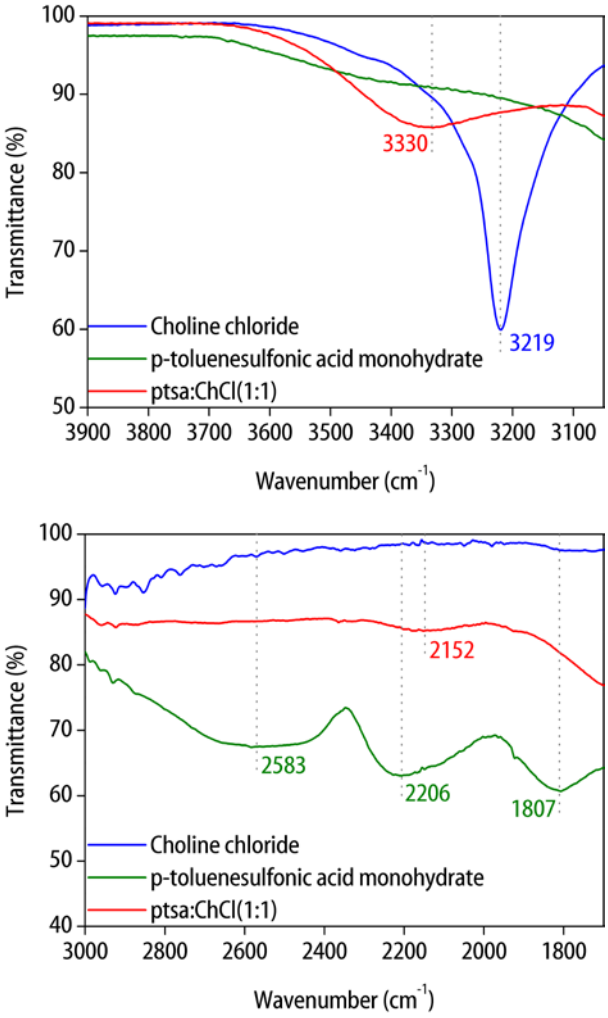

Figure 8: IR spectra of the OH stretch region (top) and of the H_3O^+ diffuse absorption region (bottom) for choline chloride (blue), *p*-toluenesulfonic acid (green) and the DES ptsa:ChCl(1:1) (red).

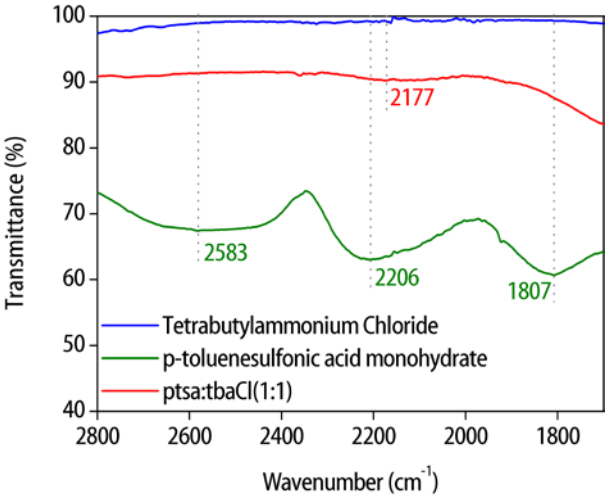

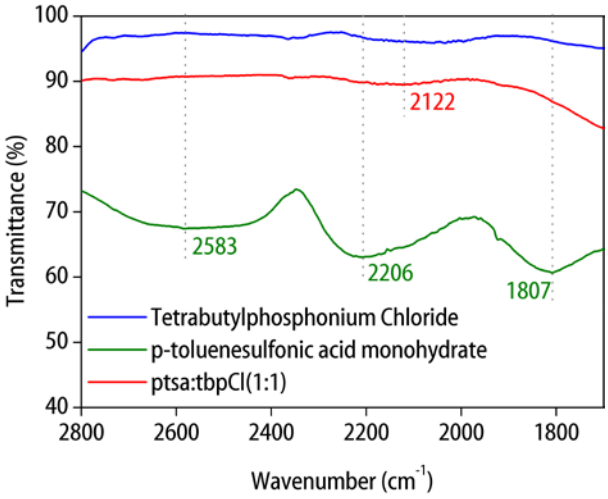

Figure 9: IR spectra of the H_3O^+ diffuse absorption region for tetrabutylammonium chloride (blue), *p*-toluenesulfonic acid (green) and the DES ptsa:tbaCl(1:1) (red) at the top; and tetrabutylphosphonium chloride (blue), *p*-toluenesulfonic acid (green) and the DES ptsa:tbaCl(1:1) (red) at the bottom.

Based on the experimentally determined physicochemical properties of the three ptsa-based DESs, ptsa:ChCl was selected as the most suitable HBD:HBA combination for the solubilization of metal oxides. The lower viscosity and broader thermal operational window were the main reason for its selection. Moreover, from an economic point of view, choline chloride is the most competitive HBA among the investigated ones. Both ptsa and ChCl are produced at industrial scale, and since DESs are considered as a mixture of two compounds, instead of as a new compound, no investments for their registration are required. The effect of the HBD:HBA molar ratio on the solubilization of metals oxides will be considered; therefore, the ptsa:ChCl mixture has been characterized at different molar ratios, i.e., ptsa:ChCl(1:2), ptsa:ChCl(1:1), and ptsa:ChCl(2:1).

Solubility of metal oxides

The solubility of different metal oxides, specifically MnO, MnO_2, Fe_2O_3, Fe_3O_4, Co_3O_4, CuO, Cu_2O, ZnO, In_2O_3, PbO, PbO_2, in the DES ptsa:ChCl was determined at 50 °C and atmospheric pressure. The effect of the HBD:HBA molar ratio (i.e., 2:1, 1:1, and 1:2) on the solubility of the metal oxides was investigated for the first time. The obtained solubility values are depicted in Figure 10, and tabulated in Table S5.

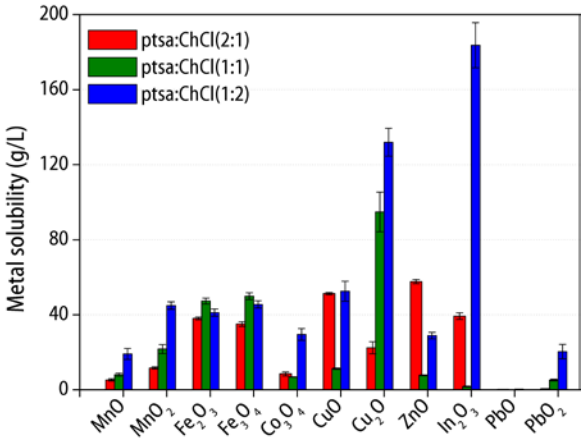

Figure 10: Metal content after solubilization of metal oxides in the deep-eutectic solvent ptsa:ChCl at different HBD:HBA molar ratios at 50 °C and atmospheric pressure.

From Figure 10, it can be observed that Cu_2O and In_2O_3 are outstandingly soluble in ptsa:ChCh(1:2) (more than 100 g/L) and also that the solubility of PbO is negligible, independently of the HBD:HBA ratio used. The effect of the HBD:HBA ratio on the solubility of the metal oxides was found to be remarkable. For example, the solubility of In_2O_3, CuO, and ZnO in ptsa:ChCl(1:2) is much higher than in ptsa:ChCl(1:1); 100, 5 and 4 times, respectively. Besides, it was observed that the highest solubilities were not always obtained for the same HBD:HBA molar ratio, but different types of behaviors have been found: (1) for MnO, MnO_2, Cu_2O and PbO the solubility decreased in the following order: ptsa:ChCl(1:2) > ptsa:ChCl(1:1) > ptsa:ChCl(2:1); (2) for In_2O_3, Co_3O_4 and CuO the higher solubilities were also obtained using ptsa:ChCl(1:2); but in this case the solubility decreased in the following order: ptsa:ChCl(1:2) > ptsa:ChCl(2:1) > ptsa:ChCl(1:1), i.e., the HBD:HBA equimolar mixture led to the lower solubilities; (3) in the case of Fe oxides, both showed a different behavior compared to the rest of the metal oxides, i.e., the highest solubility was obtained using ptsa:ChCl(1:1), followed by ptsa:ChCl(1:2) and ptsa:ChCl(2:1); and (4) ZnO was the only metal showing higher solubility in ptsa:ChCh(2:1) than in the other investigated molar ratios. According to our initial hypothesis, it would be expected that the most acidic DES (ptsa:ChCl(2:1)) would lead to the highest solubilities. Besides, ptsa:ChCl(2:1) was also found to have the lowest viscosity among all the investigated DESs, which should avoid any possible mass transfer limitation. However, in most of the cases the (2:1) molar ratio lead to the lowest metal oxides solubilities, probably meaning that the obtained results are a combination between both chemical and physical effects.

Therefore, additional research is required to further understand the behavior of these type of systems; although, the fact that we can control the solubility of the metals oxides by modifying the HBD:HBA molar ratio brings new possibilities in the field of solvometallurgy. It could be expected to find similar behaviors for other DESs, which could be potentially exploited for the development of highly selective leaching processes.

Comparison of the obtained results

A comparison between the solubility values obtained for ptsa:ChCl(1:2), malonic acid:ChCl(1:1), urea:ChCl(2:1), and an aqueous solution of HCl 3.14 M is shown in Figure 11. The concentration of the aqueous solution was chosen to match the pH of the malonic acid:ChCl(1:1), which at the moment was the best performing DES.[17] It can be observed that the solubilities obtained for ptsa:ChCl(1:2) are higher than those reported for malonic acid:ChCl(1:1), and for urea:ChCl(2:1) (which are almost negligible). In our initial hypothesis we stated that a higher acidity of the HBD would lead to a higher solubility of metal oxides, and the experimental results have confirmed this theory. However, it is worth mentioning that this is only true when the solubility data for ptsa:ChCl(1:2) are chosen for the comparison. If other HBD:HBA molar ratio was used for the comparison, the solubilities will not be always higher than those of malonic acid:ChCl(1:1). Moreover, it could also be expected that a modification of the malonic acid:ChCl molar ratio would lead to other solubility values, maybe higher. Therefore, based on the experimental results it cannot be concluded that the acidity of the HBD is the main reason for the higher metal oxides solubilities. On the contrary, it has been found that the HBD:HBA molar ratio has a greater effect on the solubility of metal oxides than the type of acid used as HBD. When the solubilities of metal oxides in ptsa:ChCl(1:2) and in HCl aqueous solutions are compared, it is observed that MnO_2, Fe_2O_3, Fe_3O_4 and CuO, are more soluble in the ptsa-based DES than in the HCl aqueous solution. Besides, compared to aqueous HCl solutions, DESs are more selective towards certain metals, depending on the chosen HBD:HBA molar ratio. This may be of great interest for the valorization of low grade ores.[1] The recovery of the metals from the DES plays a crucial role in the feasibility of the dissolution process. Successful recovery of metals from loaded DESs via electrodeposition and solvent extraction has already been reported in the literature.[54–57]

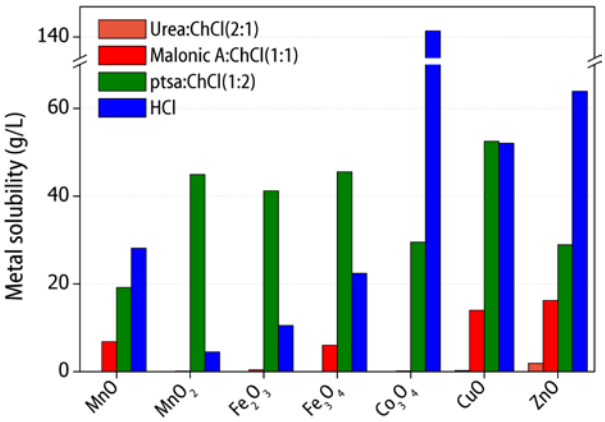

Figure 11: Solubility of metal oxides in different DESs: ptsa:ChCl(1:1), malonic acid:ChCl(1:1), urea:ChCl(2:1), ethylene glycol:ChCl(2:1) and HC at 3.14 M.[17]

Conclusions

Combinations of *p*-toluenesulfonic acid monohydrate with different HBAs were tested for DES formation, resulting in two new DESs: (1) ptsa:tetrabutylammonium chloride(1:1), and (2) ptsa:tetrabutylphosphonium chloride (1:1). The physicochemical properties (i.e., density, viscosity, decomposition temperature, melting point, IR spectroscopy) of the newly reported DESs were determined. The DES ptsa:ChCl(1:1) was found to have a lower viscosity and a larger thermal operational window compared to ptsa:tbaCl and ptsa:tbpCl. The solubility of MnO, MnO_2, Fe_2O_3, Fe_3O_4, Co_3O_4, CuO, Cu_2O, ZnO, In_2O_3, PbO, and PbO_2 in the DESs ptsa:ChCl(2:1), ptsa:ChCl(1:1), and ptsa:ChCl(1:2) was measured. The solubilities of metal oxides in ptsa:ChCl(1:2) were found to be higher than in any of the previously reported DESs. Besides, for the first time the effect of the HBD:HBA molar ratio has been investigated, and it was found that it plays a crucial role on the solubility of metal oxides. Although the effect of the HBD:HBA molar ratio is different for each metal, in most of the cases a higher ChCl concentration leads to higher solubilities. Moreover, the selectivity of the DESs can be modified by changing the HBD:HBA molar ratio. This is of potential value for the valorization of low grade ores or metal processing residues.[1] It could be expected that other type of sulfonic acid-based DESs will also lead to high metal oxides solubilities, which is important because cheaper HBDs might be used, e.g., methanesulfonic acid.

Associated content

Supporting Information:

Viscosity and density data, FTIR spectra and solubility data for metal oxides.

Author information:

Corresponding Author

*K. Binnemans. Email: Koen.Binnemans@kuleuven.be Phone: +3216327446.

ORCID

- Nerea Rodriguez Rodriguez: 0000-0002-5856-3442
- Lieven Machiels: 0000-0002-0371-424X
- Koen Binnemans: 0000-0003-4768-3606

Notes

The authors declare no competing financial interest.

Acknowledgements

The authors of this work acknowledge the Strategic Initiative Materials in Flanders (SIM) for the financial support (SBO-SMART: Sustainable Metal Extraction from Tailings) with Grant nr. HBC.2016.0456.

References

(1) Binnemans, K.; Jones, P. T. Solvometallurgy: An Emerging Branch of Extractive Metallurgy. *J. Sustain. Metall.* **2017**, *3* (3), 570–600. DOI 10.1007/s40831-017-0128-2.

(2) Batchu, N. K.; Vander Hoogerstraete, T.; Banerjee, D.; Binnemans, K. Separation of Rare-Earth Ions from Ethylene Glycol (+LiCl) Solutions by Non-Aqueous Solvent Extraction with Cyanex 923. *RSC Adv.* **2017**, *7* (72), 45351–45362. DOI 10.1039/C7RA09144C.

(3) Li, Z.; Li, X.; Raiguel, S.; Binnemans, K. Separation of Transition Metals from Rare Earths by Non-Aqueous Solvent Extraction from Ethylene Glycol Solutions Using Aliquat 336. *Sep. Purif. Technol.* **2018**, *201*, 318–326. DOI 10.1016/j.seppur.2018.03.022.

(4) Batchu, N. K.; Vander Hoogerstraete, T.; Banerjee, D.; Binnemans, K. Non-Aqueous Solvent Extraction of Rare-Earth Nitrates from Ethylene Glycol to n-Dodecane by Cyanex 923. *Sep. Purif. Technol.* **2017**, *174*, 544–553. DOI 10.1016/j.seppur.2016.10.039.

(5) Abbott, A. P.; Al-Bassam, A. Z. M.; Goddard, A.; Harris, R. C.; Jenkin, G. R. T.; Nisbet, F. J.; Wieland, M. Dissolution of Pyrite and Other Fe-S-As Minerals Using Deep Eutectic Solvents. *Green Chem.* **2017**, *19* (9), 2225–2233. DOI 10.1039/C7GC00334J.

(6) Hartley, J. M. *Ionometallurgy: The Processing of Metals Using Ionic Liquids*; University of Leicester, 2013.

(7) Abbott, A. P.; Collins, J.; Dalrymple, I.; Harris, R. C.; Mistry, R.; Qiu, F.; Scheirer, J.; Wise, W. R. Processing of Electric Arc Furnace Dust Using Deep Eutectic Solvents. *Aust. J. Chem.* **2009**, *62* (4), 341–347.

(8) Abbott, A. P.; Frisch, G.; Gurman, S. J.; Hillman, A. R.; Hartley, J.; Holyoak, F.; Ryder, K. S. Ionometallurgy: Designer Redox Properties for Metal Processing. *Chem. Commun.* **2011**, *47* (36), 10031–10033. DOI 10.1039/C1CC13616J.

(9) Abbott, A. P.; Frisch, G.; Hartley, J.; Ryder, K. S. Processing of Metals and Metal Oxides Using Ionic Liquids. *Green Chem.* **2011**, *13* (3), 471–481. DOI 10.1039/C0GC00716A.

(10) Nockemann, P.; Thijs, B.; Parac-Vogt, T. N.; Van Hecke, K.; Van Meervelt, L.; Tinant, B.; Hartenbach, I.; Schleid, T.; Ngan, V. T.; Nguyen, M. T.; et al. Carboxyl-Functionalized Task-Specific Ionic Liquids for Solubilizing Metal Oxides. *Inorg. Chem.* **2008**, *47* (21), 9987–9999. DOI 10.1021/ic801213z.

(11) Nockemann, P.; Thijs, B.; Pittois, S.; Thoen, J.; Glorieux, C.; Van Hecke, K.; Van Meervelt, L.; Kirchner, B.; Binnemans, K. Task-Specific Ionic Liquid for Solubilizing Metal Oxides. *J. Phys. Chem. B* **2006**, *110* (42), 20978–20992. DOI 10.1021/jp0642995.

(12) Davris, P.; Balomenos, E.; Panias, D.; Paspaliaris, I. Selective Leaching of Rare Earth Elements from Bauxite Residue (Red Mud), Using a Functionalized Hydrophobic Ionic Liquid. *Hydrometallurgy* **2016**, *164*, 125–135. DOI 10.1016/j.hydromet.2016.06.012.

(13) Dupont, D.; Raiguel, S.; Binnemans, K. Sulfonic Acid Functionalized Ionic Liquids for Dissolution of Metal Oxides and Solvent Extraction of Metal Ions. *Chem. Commun.* **2015**, *51* (43), 9006–9009. DOI 10.1039/C5CC02731D.

(14) Dupont, D.; Binnemans, K. Antimony Recovery from the Halophosphate Fraction in Lamp Phosphor Waste: A Zero-Waste Approach. *Green Chem.* **2016**, *18* (1), 176–185. DOI 10.1039/C5GC01746G.

(15) Dupont, D.; Binnemans, K. Recycling of Rare Earths from NdFeB Magnets Using a Combined Leaching/Extraction System Based on the Acidity and Thermomorphism of the Ionic Liquid [Hbet][Tf2N]. *Green Chem.* **2015**, *17* (4), 2150–2163. DOI 10.1039/C5GC00155B.

(16) Dupont, D.; Binnemans, K. Rare-Earth Recycling Using a Functionalized Ionic Liquid for the Selective Dissolution and Revalorization of Y2O3:Eu3+ from Lamp Phosphor Waste. *Green Chem.* **2015**, *17* (2), 856–868. DOI 10.1039/C4GC02107J.

(17) Abbott, A. P.; Capper, G.; Davies, D. L.; McKenzie, K. J.; Obi, S. U. Solubility of Metal Oxides in Deep Eutectic Solvents Based on Choline Chloride. *J. Chem. Eng. Data* **2006**, *51* (4), 1280–1282. DOI 10.1021/je060038c.

(18) Abbott, A. P.; Capper, G.; Davies, D. L.; Rasheed, R. K.; Shikotra, P. Selective Extraction of Metals from Mixed Oxide Matrixes Using Choline-Based Ionic Liquids. *Inorg. Chem.* **2005**, *44* (19), 6497–6499. DOI 10.1021/ic0505450.

(19) Abbott, A. P.; Boothby, D.; Capper, G.; Davies, D. L.; Rasheed, R. K. Deep Eutectic Solvents Formed between Choline Chloride and Carboxylic Acids: Versatile Alternatives to Ionic Liquids. *J. Am. Chem. Soc.* **2004**, *126* (29), 9142–9147. DOI 10.1021/ja048266j.

(20) Otto, L.; Lars, R. Benzenesulfonic Acids and Their Derivatives. In *Ullmann's Encyclopedia of Industrial Chemistry*; American Cancer Society, 2000. DOI 10.1002/14356007.a03_507.

(21) von Rymon Lipinski Gert-Wolfhard. Sweeteners. In *Ullmann's Encyclopedia of Industrial Chemistry*; American Cancer Society, 2015; pp 1–25. DOI 10.1002/14356007.a26_023.pub2.

(22) J C, W.; B H, W.; D L, Z.; G F, S.; J T, Y.; B F, L. Production of P-toluenesulfonic Acid by Sulfonating Toluene with Gaseous Sulfur Trioxide. *J. Chem. Technol. Biotechnol.* **2001**, *76* (6), 619–623. DOI 10.1002/jctb.425.

(23) Taysun, M. B.; Sert, E.; Atalay, F. S. Physical Properties of Benzyl Tri-Methyl Ammonium Chloride Based Deep Eutectic Solvents and Employment as Catalyst. *J. Mol. Liq.* **2016**, *223*, 845–852. DOI 10.1016/j.molliq.2016.07.148.

(24) Assanosi, A. A.; Farah, M. M.; Wood, J.; Al-Duri, B. A Facile Acidic Choline Chloride-p-TSA DES-Catalysed Dehydration of Fructose to 5-Hydroxymethylfurfural. *RSC Adv.* **2014**, *4* (74), 39359–39364. DOI 10.1039/C4RA07065H.

(25) Hayyan, A.; Ali Hashim, M.; Mjalli, F. S.; Hayyan, M.; AlNashef, I. M. A Novel Phosphonium-Based Deep Eutectic Catalyst for Biodiesel Production from Industrial Low Grade Crude Palm Oil. *Chem. Eng. Sci.* **2013**, *92*, 81–88. DOI 10.1016/j.ces.2012.12.024.

(26) Hayyan, A.; Hashim, M. A.; Hayyan, M.; Mjalli, F. S.; AlNashef, I. M. A New Processing Route for Cleaner Production of Biodiesel Fuel Using a Choline Chloride Based Deep Eutectic Solvent. *J. Clean. Prod.* **2014**, *65*, 246–251. DOI 10.1016/j.jclepro.2013.08.031.

(27) Wang, L.; Zhong, X.; Zhou, M.; Zhou, W.; Chen, Q.; He, M.-Y. One-Pot Synthesis of Polysubstituted Imidazoles in a Br?Nsted Acidic Deep Eutectic Solvent. *J. Chem. Res.* **2013**, *37* (4). DOI 10.3184/174751913X13636339694414.

(28) De Santi, V.; Cardellini, F.; Brinchi, L.; Germani, R. Novel Brønsted Acidic Deep Eutectic Solvent as Reaction Media for Esterification of Carboxylic Acid with Alcohols. *Tetrahedron Lett.* **2012**, *53* (38), 5151–5155. DOI 10.1016/j.tetlet.2012.07.063.

(29) Yin, J.; Wang, J.; Li, Z.; Li, D.; Yang, G.; Cui, Y.; Wang, A.; Li, C. Deep Desulfurization of Fuels Based on an Oxidation/Extraction Process with Acidic Deep Eutectic Solvents. *Green Chem.* **2015**, *17* (9), 4552–4559. DOI 10.1039/C5GC00709G.

(30) Hashim, S. N. R. and A. H. and M. A. Production of Fatty Acid Methyl Ester from Low Grade Palm Oil Using Eutectic Solvent Based on Benzyltrimethylammonium Chloride. *IOP Conf. Ser. Mater. Sci. Eng.* **2017**, *210* (1), 12012.

(31) Cui, Y.; Li, C.; Yin, J.; Li, S.; Jia, Y.; Bao, M. Design, Synthesis and Properties of Acidic Deep Eutectic Solvents Based on Choline Chloride. *J. Mol. Liq.* **2017**, *236*, 338–343. DOI 10.1016/j.molliq.2017.04.052.

(32) Zhao, B.-Y.; Xu, P.; Yang, F.-X.; Wu, H.; Zong, M.-H.; Lou, W.-Y. Biocompatible Deep Eutectic Solvents Based on Choline Chloride: Characterization and Application to the Extraction of Rutin from Sophora Japonica. *ACS Sustain. Chem. Eng.* **2015**, *3* (11), 2746–2755. DOI 10.1021/acssuschemeng.5b00619.

(33) Sirviö, J. A.; Visanko, M.; Liimatainen, H. Acidic Deep Eutectic Solvents As Hydrolytic Media for Cellulose Nanocrystal Production. *Biomacromolecules* **2016**, *17* (9), 3025–3032. DOI 10.1021/acs.biomac.6b00910.

(34) Montalbán, M. G.; Bolívar, C. L.; Díaz Baños, F. G.; Víllora, G. Effect of Temperature, Anion, and Alkyl Chain Length on the Density and Refractive Index of 1-Alkyl-3-Methylimidazolium-Based Ionic Liquids. *J. Chem. Eng. Data* **2015**, *60* (7), 1986–1996. DOI 10.1021/je501091q.

(35) García, G.; Aparicio, S.; Ullah, R.; Atilhan, M. Deep Eutectic Solvents: Physicochemical Properties and Gas Separation Applications. *Energy & Fuels* **2015**, *29* (4), 2616–2644. DOI 10.1021/ef5028873.

(36) Rodriguez, N. R. *Azeotrope Breaking Using Deep Eutectic Solvents*; Eindhoven: Technische Universiteit Eindhoven, 2016.

(37) Rodriguez, N. R.; Ferre Guell, J.; Kroon, M. C. Glycerol-Based Deep Eutectic Solvents as Extractants for the Separation of MEK and Ethanol via Liquid–Liquid Extraction. *J. Chem. Eng. Data* **2016**, *61* (2), 865–872. DOI 10.1021/acs.jced.5b00717.

(38) Shirota, H.; Fukazawa, H.; Fujisawa, T.; Wishart, J. F. Heavy Atom Substitution Effects in Non-Aromatic Ionic Liquids: Ultrafast Dynamics and Physical Properties. *J. Phys. Chem. B* **2010**, *114* (29), 9400–9412. DOI 10.1021/jp1021104.

(39) Carvalho, P. J.; Ventura, S. P. M.; Batista, M. L. S.; Schröder, B.; Gonçalves, F.; Esperança, J.; Mutelet, F.; Coutinho, J. A. P. Understanding the Impact of the Central Atom on the Ionic Liquid Behavior: Phosphonium vs Ammonium Cations. *J. Chem. Phys.* **2014**, *140* (6), 64505. DOI 10.1063/1.4864182.

(40) Griffin, P. J.; Holt, A. P.; Tsunashima, K.; Sangoro, J. R.; Kremer, F.; Sokolov, A. P. Ion

Transport and Structural Dynamics in Homologous Ammonium and Phosphonium-Based Room Temperature Ionic Liquids. *J. Chem. Phys.* **2015**, *142* (8), 84501. DOI 10.1063/1.4913239.

(41) Florindo, C.; Oliveira, F. S.; Rebelo, L. P. N.; Fernandes, A. M.; Marrucho, I. M. Insights into the Synthesis and Properties of Deep Eutectic Solvents Based on Cholinium Chloride and Carboxylic Acids. *ACS Sustain. Chem. Eng.* **2014**, *2* (10), 2416–2425. DOI 10.1021/sc500439w.

(42) María, F.; Adriaan, van den B.; C., K. M. Low-Transition-Temperature Mixtures (LTTMs): A New Generation of Designer Solvents. *Angew. Chemie Int. Ed.* **2013**, *52* (11), 3074–3085. DOI 10.1002/anie.201207548.

(43) Brown, R. J. C.; Brown, R. F. C. Melting Point and Molecular Symmetry. *J. Chem. Educ.* **2000**, *77* (6), 724. DOI 10.1021/ed077p724.

(44) Zhao, H. Review: Current Studies on Some Physical Properties of Ionic Liquids. *Phys. Chem. Liq.* **2003**, *41* (6), 545–557. DOI 10.1080/0031910310001173l9.

(45) Perkins, S. L.; Painter, P.; Colina, C. M. Molecular Dynamic Simulations and Vibrational Analysis of an Ionic Liquid Analogue. *J. Phys. Chem. B* **2013**, *117* (35), 10250–10260. DOI 10.1021/jp404619x.

(46) Perkins, S. L.; Painter, P.; Colina, C. M. Experimental and Computational Studies of Choline Chloride-Based Deep Eutectic Solvents. *J. Chem. Eng. Data* **2014**, *59* (11), 3652–3662. DOI 10.1021/je500520h.

(47) Krasovskii, A. N.; Kalnin'sh, K. K. IR Spectra of Long-Chain Alkylsulfonic Acids. *J. Appl. Spectrosc.* **1977**, *26* (6), 745–749. DOI 10.1007/BF01124478.

(48) Pejov, L.; Ristova, M.; Šoptrajanov, B. Quantum Chemical Study of P-Toluenesulfonic Acid, p-Toluenesulfonate Anion and the Water–p-Toluenesulfonic Acid Complex. Comparison with Experimental Spectroscopic Data. *Spectrochim. Acta Part A* **2011**, *79* (1), 27–34. DOI 10.1016/j.saa.2011.01.007.

(49) Ristova, M.; Pejov, L.; Žugić, M.; Šoptrajanov, B. Experimental IR, Raman and Ab Initio Molecular Orbital Study of the 4-Methylbenzenesulfonate Anion. *J. Mol. Struct.* **1999**, *482–483*, 647–651. DOI 10.1016/S0022-2860(98)00890-4.

(50) Anastassopoulou, J. D. Mass and FT-IR Spectra of Quaternary Ammonium Surfactants BT - Chemistry and Properties of Biomolecular Systems; Rizzarelli, E., Theophanides, T., Eds.; Springer Netherlands: Dordrecht, 1991; pp 1–9. DOI 10.1007/978-94-011-3620-4_1.

(51) Kleeberg, H. IR-Spectroscopic Investigation of the Hydration of Tetrabutylammonium Bromide in Methylene Chloride. *J. Solution Chem.* **1986**, *15* (2), 169–176. DOI 10.1007/BF00646288.

(52) Gorman, M. The Evidence from Infrared Spectroscopy for Hydrogen Bonding: A Case History of the Correlation and Interpretation of Data. *J. Chem. Educ.* **1957**, *34* (6), 304–306. DOI 10.1021/ed034p304.

(53) Spectral Analysis. In *Infrared Spectroscopy: Fundamentals and Applications*; Wiley-Blackwell, 2005; pp 45–70. DOI 10.1002/0470011149.ch3.

(54) Bučko, M.; Culliton, D.; Betts, A. J.; Bajat, J. B. The Electrochemical Deposition of Zn–Mn Coating from Choline Chloride–urea Deep Eutectic Solvent. *Trans. IMF* **2017**, *95* (1), 60–64. DOI 10.1080/00202967.2017.1255412.

(55) Abbott, A. P.; Alhaji, A. I.; Ryder, K. S.; Horne, M.; Rodopoulos, T. Electrodeposition of Copper–tin Alloys Using Deep Eutectic Solvents. *Trans. IMF* **2016**, *94* (2), 104–113. DOI 10.1080/00202967.2016.1148442.

(56) Alcanfor, A. A. C.; dos Santos, L. P. M.; Dias, D. F.; Correia, A. N.; de Lima-Neto, P. Electrodeposition of Indium on Copper from Deep Eutectic Solvents Based on Choline Chloride and Ethylene Glycol. *Electrochim. Acta* **2017**, *235*, 553–560. DOI 10.1016/j.electacta.2017.03.082.

(57) Riano, S.; Petranikova, M.; Onghena, B.; Vander Hoogerstraete, T.; Banerjee, D.; Foreman, M. R. S.; Ekberg, C.; Binnemans, K. Separation of Rare Earths and Other Valuable Metals from Deep-Eutectic Solvents: A New Alternative for the Recycling of Used NdFeB Magnets. *RSC Adv.* **2017**, *7* (51), 32100–32113. DOI 10.1039/C7RA06540J.

TOC graph

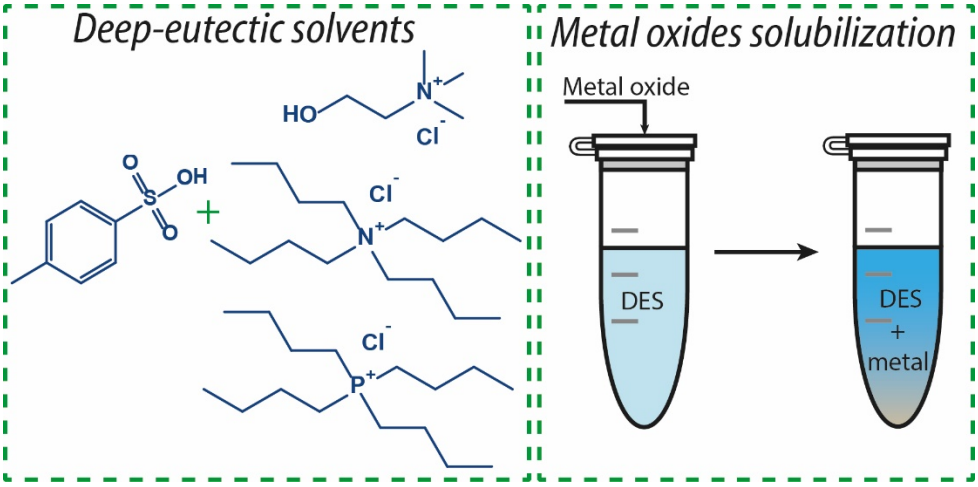

Synopsis

Highly acidic deep-eutectics solvents based on *p*-toluenesulfonic acid have been prepared, characterized, and tested for solubilization of metal oxides.